Reed-Solomon codes implementing a coded Single-Carrier with Cyclic Prefix scheme

Geert Van Meerbergen, *Member, IEEE,* Marc Moonen, *Fellow, IEEE,* and Hugo De Man, *Fellow, IEEE*

***Abstract*— This paper presents a novel Reed-Solomon codes based transmission scheme called RS-SC-CP. While RS-SC-CP is essentially a Reed-Solomon (RS) coded single carrier with cyclic prefix (SC-CP) system, a filter bank representation of the RS code is used. This filter bank representation unveils a DFT synthesis bank, just as in a traditional Orthogonal Frequency Division Multiplexing (OFDM) system (allbeit in a finite field). Therefore, RS-SC-CP is topologically equivalent with OFDM. As such, the RS-SC-CP system inherits the advantages of an SC-CP system over a traditional OFDM system like a low Peak to Average Power Ratio (PAPR). But, more importantly, it allows us to use a novel equalization technique that resembles a traditional OFDM equalizer. The equalizer of an RS-SC-CP receiver is split into two stages: the first stage encompasses a partial equalization in the complex field, which ensures that the residual channel response has integer coefficients. It is calculated using a Minimum Mean Square Error (MMSE) criterion. The residual ISI is removed by a *Galois field equalizer* in the second stage, *posterior* to the RS decoding removing the noise.**

Finally, the performance of the RS-SC-CP system is further evaluated by simulations showing the performance gain of the RS-SC-CP system compared to a traditional coded OFDM or Single Carrier with Cyclic Prefix (SC-CP) scheme.

I. Introduction

THE RS-SC-CP scheme presented in this paper is a novel SC-CP communication scheme that combines Reed-Solomon (RS) codes with concepts drawn from Orthogonal Frequency Division Multiplexing (OFDM). RS-SC-CP is based on a critically subsampled filter bank representation of the RS code. The DFT-like synthesis bank of such a filter bank representation resembles an OFDM modulator, allbeit in the finite field. Therefore, the newly proposed RS-SC-CP system does not suffer from a high Peak to Average Power Ratio (PAPR) as a regular OFDM system will do. Secondly, due to the seamless integration of a finite field DFT and the RS code, the system solves another shortcoming of OFDM: its lack of frequency diversity. Designing a good error correcting code for a traditional OFDM system is not an easy task. Finally, due its topological equivalence with OFDM, a novel two stage equalizer will be developed. Note that due the Galois field DFT operation, the system can be seen to be a mix between a SC-CP system (e.g. with the transmitted symbols belonging to a PAM/QAM constellation) and an OFDM system (due to the DFT synthesis bank and the second stage of the equalizer, which resembles an OFDM-like frequency domain equalization).

The key concept behind RS-SC-CP is a critically subsampled filter bank representation of an RS code which was developed earlier [5], [6]. The synthesis bank of this filter bank unveils a Galois field DFT, which is not very surprising seen the strong link between RS codes and the DFT. Frequency domain encoding of RS codes is very well known, see e.g. [7]. Such a frequency domain encoder for $\mathcal{R}(\nu, \kappa)$ can be represented in a straightforward manner as a filter bank with ν bands, subsampled with ν. The condition for this filter bank to implement an RS code is also simple: $\nu - \kappa$ adjacent subbands contain a zero, and hence can be erased. The disadvantage of using such a filter bank in an RS-SC-CP scheme is that the codeword length ν equals the OFDM block length (size of the DFT). Therefore, this paper calls upon a more advanced filter bank structure of an RS code in which a codeword (length ν) consists of multiple OFDM blocks of size M. M is then also the subsampling factor.

Mitigating the disadvantages while inheriting the advantages of SC-CP and OFDM, RS-SC-CP seems a powerful candidate for broadband wireless and wire-line communications.

While our paper [1] focuses on impulse noise scenario's with fixed channels, this paper addresses performance issues of RS-SC-CP in Rayleigh fading channels with Additive White Gaussian Noise (AWGN). The most important aspect in this context is the addition of a complex field equalizer preceding the RS decoder. In this paper, an MMSE based method is given to design the complex field equalizer coefficients.

The paper is organized as follows. The first section briefly explains RS-SC-CP and gives an instructive example. Section III discusses how the characteristics of a non-integer fading channel with AWGN can be accommodated within the RS-SC-CP system. The last section compares the RS-SC-CP system with a traditional coded OFDM and a Single Carrier with Cyclic Prefix (SC-CP) system.

Notation: Lower/upper case bold-face symbols represent vectors/matrices, respectively. The Z-transform of a vector $\mathbf{a} = \begin{bmatrix} a(0) & a(1) & a(2) & \dots \end{bmatrix}^T$ is represented by $A(z^{-1}) = a(0) + a(1)z^{-1} + a(2)z^{-2} + \dots$. The m-th polyphase component of order M is denoted as $\mathbf{a}_m^{[M]} = \begin{bmatrix} a(m) & a(m+M) & a(m+2M) & \dots \end{bmatrix}^T$ ($A_m^{[M]}(z^{-1})$ in the Z-domain). The $M \times 1$ vector of or-

This paper was presented in part at the IEEE Global Telecommunications Conference (GLOBECOM), San Francisco, USA, Nov. 27 - Dec. 1, 2006.

Geert Van Meerbergen is a Research Assistant with the F.W.O. Vlaanderen. This research work was carried out at the ESAT laboratory of the Katholieke Universiteit Leuven, in the frame of the Interuniversity Poles of Attraction Programme P5/11

G. Van Meerbergen and M. Moonen are with the EE Dept. (ESAT), K.U.Leuven, Kasteelpark Arenberg 10, B-3001 Leuven, Belgium (e-mail: geert.vanmeerbergen@esat.kuleuven.be; marc.moonen@esat.kuleuven.be).

H. De Man is with IMEC, Kapeldreef 75, B-3001 Leuven, Belgium (e-mail: hugo.deman@imec.be). H. De Man is also with the EE Dept. (ESAT), K.U.Leuven, Belgium.

der M polyphase components is denoted as $\mathbf{A}^{[M]}(z^{-1}) = \left[A_0^{[M]}(z^{-1}) \quad A_1^{[M]}(z^{-1}) \quad \dots \quad A_{M-1}^{[M]}(z^{-1})\right]^T$.

II. RS-SC-CP

A block scheme of an RS-SC-CP system is shown in Figure 1. The filter bank structure in the transmitter implements an RS code $\mathcal{R}(\nu,\kappa)$ in $GF(p^d)$ ($\nu = p^d - 1$), as will now be explained. For a detailed description of the equivalence between filter banks and RS codes, the interested reader is referred to [5], [6]. A dataword of κ GF symbols $\underline{U}(z^{-1})$ is split into its M polyphase components $\underline{U}_0^{[M]}(z^{-1}) \dots \underline{U}_{M-1}^{[M]}(z^{-1})$. For the sake of easy mathematics, we first assume κ and M are not coprime such that each polyphase component has $\kappa' = \frac{\kappa}{M}$ symbols [5]. Redundancy is added to each polyphase component $\underline{U}_m^{[M]}(z^{-1})$ by a terminated convolutional code $\underline{D}_m(z^{-1})$ of rate $\frac{\kappa}{\nu}$:

$$\underline{X}_m^{[M]}(z^{-1}) = \underline{D}_m^{[M]}(z^{-1})\underline{U}_m^{[M]}(z^{-1}) \tag{1}$$

The design of these subband codes is critical. With α a primitive ν-th root of unity, the consecutive roots of the RS code $\mathcal{R}(\nu,\kappa)$ α^i, $i = 0 \dots \nu - \kappa + 1$, are distributed among the subband codes as

$$\underline{D}_m(\alpha^i) = 0 \Leftrightarrow i \bmod M = m. \tag{2}$$

The subband codes then operate as small RS-like codes, encoding a dataword of $\kappa' = \frac{\kappa}{M}$ symbols into a codeword $\underline{X}_m^{[M]}(z^{-1})$ of $\nu' = \frac{\nu}{M}$ symbols.

The subband samples $\underline{X}_m^{[M]}(z^{-1})$ are fed into a synthesis bank with

$$\underline{C}_m(z^{-1}) \quad = \quad \sum_{m'=0}^{M-1} \underline{W}_M^{-mm'} z^{-m'} \tag{3}$$

where

$$\underline{W}_M = \alpha^{\frac{\nu}{M}} = \alpha^{\nu'} \tag{4}$$

is an M-th root of unity in the GF. Note that M should be chosen a divisor of ν for $\underline{W}_M$ to exist. In the case that κ and M are coprime, a more careful distribution of the roots is required (see [5], [6]) but essentially the same procedure holds. In the same paper, it is shown that the previously described multirate system implements the RS code $\mathcal{R}(\nu,\kappa)$. This means that the output of the filter bank

$$\underline{Y}(z^{-1}) = \sum_{m=0}^{M-1} \underline{C}_m(z^{-1})\underline{X}_m^{[M]}(z^{-M}) \tag{5}$$

is a codeword of $\mathcal{R}(\nu,\kappa)$, up to an interleaving.

From a matrix point of view, the vector of polyphase components of this codeword is obtained as

$$\underline{\mathbf{Y}}^{[\mathbf{M}]}(z^{-1}) = \underline{\mathbf{F}}_M^{-1} \text{diag}\left(\underline{\mathbf{D}}(z^{-1})\right) \underline{\mathbf{U}}^{[\mathbf{M}]}(z^{-1}) \tag{6}$$

with

$$\underline{\mathbf{F}}_M(i,j) \quad = \quad \underline{W}_M^{ij} \tag{7}$$

$$\underline{\mathbf{D}}(z^{-1}) \quad = \quad \left[\underline{D}_0(z^{-1}) \quad \dots \quad \underline{D}_{M-1}(z^{-1})\right]^T \tag{8}$$

The next step in Figure 1 consists of a specific mapping of the GF symbols onto QAM constellation points. Here, to make the mathematics more accessible, the method is illustrated with a PAM instead of a QAM constellation. Nevertheless, the same techniques hold if a mapping between $GF(p^2)$ and a p^2-QAM constellation with complex integer numbers is used. More information can be found in appendix. Choosing a GF of odd characteristic ($d = 1$), and bearing in mind the isomorphism between the symbols of $GF(p)$ and a p-PAM constellation with the integers modulo p, each codeword symbol is mapped onto its corresponding integer representation. This representation can be found starting from the primitive polynomial $s(x) = s_0 + x$ uniquely defining the GF: The primitive $p-1$-st root of unity α is a root of this primitive polynomial:

$$\alpha = -s_0 \bmod p \tag{9}$$

This equation defines the isomorphism between the elements of the GF and the integers modulo p:

$$\underline{a} = \alpha^i \leftrightarrow a = (-s_0)^i \bmod p \tag{10}$$

From a notational point of view, note that the GF representation of a (matrix) variable a is denoted by $\underline{a}$. To limit the power of the signal, it is preferred to bound the integers between $-\frac{p-1}{2} \dots \frac{p-1}{2}$ instead of $0 \dots p-1$. Hence, the modulo operation $x \bmod p$ is replaced by $(x)_p$

$$(x)_p = \text{round}\left(x - p\left\lfloor \frac{(x+\frac{p}{2})}{p} \right\rfloor\right), \tag{11}$$

such that the mapping becomes

$$\underline{a} = \alpha^i \leftrightarrow a = ((-s_0)^i)_p. \tag{12}$$

In the RS-SC-CP transmitter, Equation 12 is used to map a GF symbol $\underline{a}$ into an integer a (p-PAM symbol). At the receiver, Equations 12 and 18 will be used to map a complex valued (i.e. not necessarily integer) x back into an integer $(x)_p$ and then to a GF symbol $\underline{x}$ (which thus incorporates a decision).

Finally, as in a traditional SC-CP scenario, a cyclic prefix of length L is added to each block (size M) to convert the linear convolution of the channel $H(z^{-1}) = h(0) + h(1)z^{-1} + \dots + h(L)z^{-L}$ into a circular convolution. AWGN is added and the CP is again removed at the receiver. Let us assume that, for the rest of this section, $H(z^{-1})$ is integer valued and that the noise is *impulse noise*. In this case, the complex field equalization block in Figure 1 can be ignored. In section III, this assumption will be removed. From a matrix point of view, the polyphase components of the channel output after quantization can then be written as

$$\tilde{\mathbf{Y}}^{[\mathbf{M}]}(z^{-1}) = \left(\tilde{\mathbf{H}}\mathbf{Y}^{[\mathbf{M}]}(z^{-1}) + \mathbf{N}(z^{-1})\right)_p \tag{13}$$

with the $M \times M$ circulant channel matrix

$$\tilde{\mathbf{H}} = \begin{bmatrix} h(0) & & & h(L) & \dots & h(1) \\ h(1) & \ddots & & & \ddots & \vdots \\ \vdots & \ddots & \ddots & & & h(L) \\ h(L) & & \ddots & \ddots & & \\ & \ddots & & \ddots & \ddots & \\ & & h(L) & \dots & h(1) & h(0) \end{bmatrix} \tag{14}$$

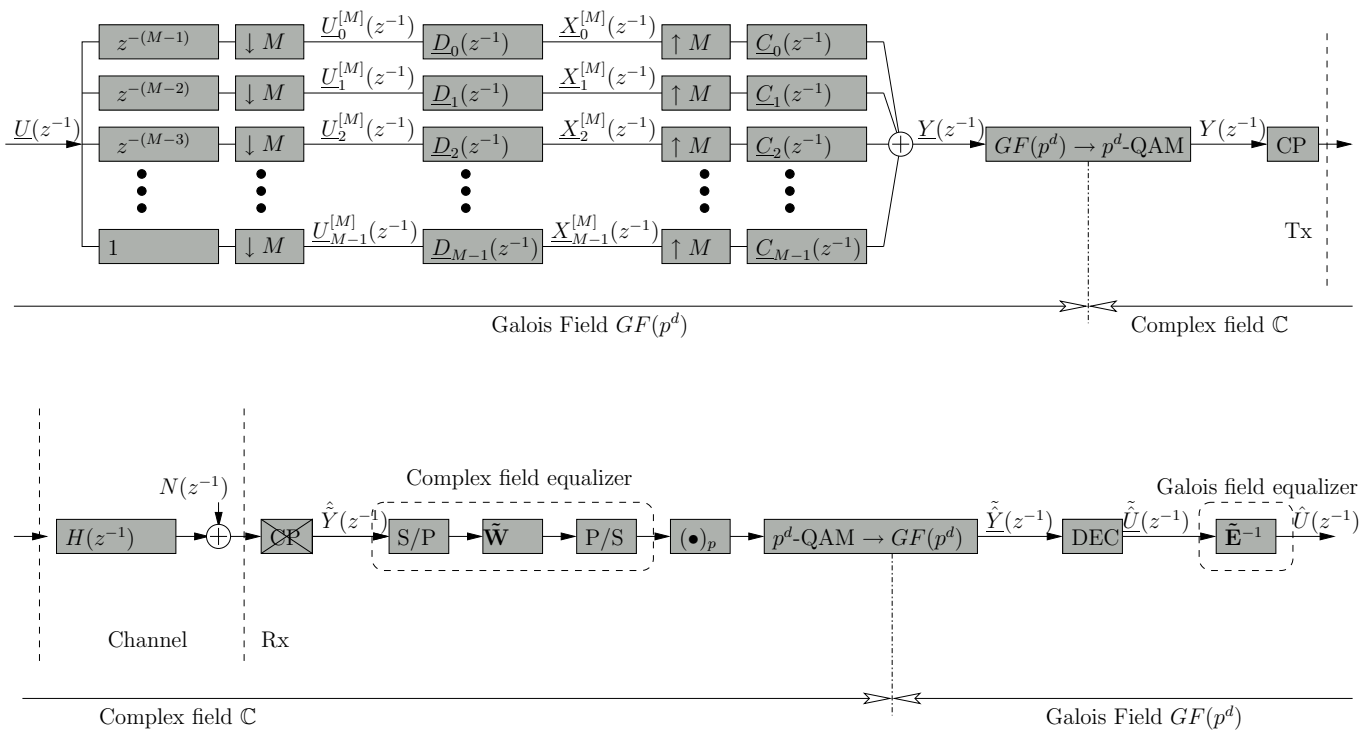

Fig. 1. Transmultiplexer structure of a baseband discrete-time model of an RS-SC-CP system.

The RS-SC-CP system can now be summarized in a few lines. The GF counterpart of Equation 13 is

$$\tilde{\underline{\mathbf{Y}}}^{[\mathbf{M}]}(z^{-1}) = \tilde{\underline{\mathbf{H}}}\underline{\mathbf{Y}}^{[M]}(z^{-1}) + \underline{\mathbf{N}}'(z^{-1}) \tag{15}$$

with $\mathbf{N}'(z^{-1}) = (\mathbf{N}(z^{-1}))_p$. Note that the modulo-like function $(x)_p$ is now called with $x \in \mathbb{R}$, and thus represents a quantization operation. The *Galois field* matrix $\tilde{\underline{\mathbf{H}}}$ can subsequently be diagonalized by *Galois field* DFT matrices

$$\tilde{\underline{\mathbf{E}}} = \underline{\mathbf{F}}_M \tilde{\underline{\mathbf{H}}} \underline{\mathbf{F}}_M^{-1} \tag{16}$$

Recalling Equation 6

$$\begin{aligned}
\tilde{\underline{\mathbf{Y}}}^{[\mathbf{M}]}(z^{-1}) &= \tilde{\underline{\mathbf{H}}}\underline{\mathbf{F}}_M^{-1}\text{diag}\left(\underline{\mathbf{D}}(z^{-M})\right)\underline{\mathbf{U}}^{[\mathbf{M}]}(z^{-1}) + \underline{\mathbf{N}}'(z^{-1}) \\
&= \underline{\mathbf{F}}_M^{-1}\tilde{\underline{\mathbf{E}}}\text{diag}\left(\underline{\mathbf{D}}(z^{-M})\right)\underline{\mathbf{U}}^{[\mathbf{M}]}(z^{-1}) + \underline{\mathbf{N}}'(z^{-1}) \\
&= \underline{\mathbf{F}}_M^{-1}\text{diag}\left(\underline{\mathbf{D}}(z^{-M})\right)\underbrace{\tilde{\underline{\mathbf{E}}}\underline{\mathbf{U}}^{[\mathbf{M}]}(z^{-1})}_{\tilde{\underline{\mathbf{U}}}^{[\mathbf{M}]}(z^{-1})} + \underline{\mathbf{N}}'(z^{-1})
\end{aligned}$$

The last equation shows that the same $\tilde{\underline{\mathbf{Y}}}^{[\mathbf{M}]}$ can be obtained by encoding a *different* dataword $\tilde{\underline{\mathbf{U}}}^{[\mathbf{M}]}$ and transmitting this over a channel $H(z^{-1}) = 1$. In other words, the channel output is also a codeword (up to the noise). This in particular leads to 2 important observations: First, the distance aimed for by the error correcting code is now preserved by the channel whereas in a typical system, the distance of the error correcting code is not preserved by the modulator, let-alone the channel. A second important observation is related to receiver design. Any RS decoder, e.g. *Berlekamp-Massey's algorithm* [8], can be applied first at the receiver to find a solution for $\tilde{\underline{\mathbf{U}}}^{[\mathbf{M}]}$, and then a GF equalization can be performed on the obtained data according to

$$\tilde{\underline{\mathbf{E}}}\underline{\mathbf{U}}^{[\mathbf{M}]}(z^{-1}) = \tilde{\underline{\mathbf{U}}}^{[\mathbf{M}]}(z^{-1}) \tag{17}$$

Note the equivalence between the latter equations and the equations describing a traditional OFDM system.

In this case, equalization and decoding are separated without compromising optimality (no joint decoding-equalization necessary) and can readily be swapped. However, if the aforementioned assumptions (integer channel, impulse noise only) are not met, a more complicated approach must be followed as discussed in section III.

Note that the quality of RS-SC-CP heavily depends on the decoding algorithm that is chosen. Berlekamp-Massey's algorithm is a bounded distance hard-decision decoder, with a performance that is inferior to a true ML hard-decision decoder. Even more powerful soft-decision algorithms [9], [10] can be used, at the expense of a higher complexity. In the latter case, the modulo block should only perform a folding of the received symbols (and not a rounding) such that soft information can be derived:

$$(x)_p = x - p\left\lfloor \frac{(x + \frac{p}{2})}{p} \right\rfloor, \tag{18}$$

However, for complexity reasons, we have chosen to use Berlekamp-Massey's algorithm in all simulations in this paper.

Example 1: For the sake of simplicity, a small GF of prime characteristic $GF(13)$ is chosen ($p = 13$) with primitive polynomial $\Pi(x) = 11 + x$. The primitive $p - 1$-st root of unity α is a root of this primitive polynomial:

$$\alpha = -11 \bmod 13 = 2$$

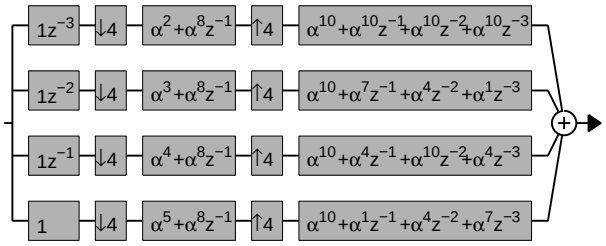

Fig. 2. Critically subsampled filter bank with $M = 4$ bands implementing $\mathcal{R}(12, 8)$ (example 1).

The isomorphism between the elements of the GF and the integers modulo 13 can now be constructed:

$$\begin{array}{cccccccccccc} 0 & 1 & \alpha^1 & \alpha^2 & \alpha^3 & \alpha^4 & \alpha^5 & \alpha^6 & \alpha^7 & \alpha^8 & \alpha^9 & \alpha^{10} & \alpha^{11} \\ \updownarrow & \updownarrow & \updownarrow & \updownarrow & \updownarrow & \updownarrow & \updownarrow & \updownarrow & \updownarrow & \updownarrow & \updownarrow & \updownarrow & \updownarrow \\ 0 & 1 & 2 & 4 & -5 & 3 & 6 & -1 & -2 & -4 & 5 & -3 & -6 \end{array}$$

We first construct a filter bank which implements $\mathcal{R}(12, 8)$ in $GF(13)$. The number of bands M should be a divisor of the codeword length $\nu = 12$, e.g. $M = 4$. Note that M can be coprime with the length of the dataword $\kappa = 8$, but to make the mathematics more tractable here, M is a divisor of κ. The roots of $\mathcal{R}(12, 8)$ are chosen $\{\alpha^k\}_{k=0\ldots3}$. Hence, each codeword is a multiple of the generator polynomial

$$\underline{G}(z^{-1}) = \prod_{k=0}^{3}(z^{-1} - \alpha^k) \tag{19}$$

These roots $\alpha^0, \alpha^1, \alpha^2, \alpha^3$ are trivially distributed among the polynomials $\underline{D}_m(z^{-1})$ as follows:

$$\begin{aligned} \alpha^0 &\Leftarrow \underline{D}_0(z^{-1}) = \alpha^2 + \alpha^8 z^{-1} \\ \alpha^1 &\Leftarrow \underline{D}_1(z^{-1}) = \alpha^3 + \alpha^8 z^{-1} \\ \alpha^2 &\Leftarrow \underline{D}_2(z^{-1}) = \alpha^4 + \alpha^8 z^{-1} \\ \alpha^3 &\Leftarrow \underline{D}_3(z^{-1}) = \alpha^5 + \alpha^8 z^{-1} \end{aligned}$$

The filter bank so obtained is shown in Figure 2. In this case, each band receives $\kappa' = 2$ dataword symbols $\underline{U}_m^{[4]}(z^{-1})$. The subband filters expand each $\underline{U}_m^{[4]}(z^{-1})$ to $\nu' = 3$ dataword symbols $\underline{X}_m^{[4]}(z^{-1})$ according to a code rate of $\frac{2}{3}$. Finally, $\underline{X}_m^{[4]}(z^{-1})$ are combined in the DFT-synthesis bank such that the output of the filter bank $\underline{Y}(z^{-1})$ is a valid RS codeword.

The synthesis bank implements a multiplication with the inverse of an M-point DFT-matrix

$$\underline{\mathbf{F}}_4^{-1} = \alpha^{10}\begin{bmatrix} 1 & 1 & 1 & 1 \\ 1 & \alpha^9 & \alpha^6 & \alpha^3 \\ 1 & \alpha^6 & 1 & \alpha^6 \\ 1 & \alpha^3 & \alpha^6 & \alpha^9 \end{bmatrix} \leftrightarrow \mathbf{F}_4^{-1} = \begin{bmatrix} -3 & -3 & -3 & -3 \\ -3 & -2 & 3 & 2 \\ -3 & 3 & -3 & 3 \\ -3 & 2 & 3 & -2 \end{bmatrix}$$

(with $\alpha^{10} = \frac{1}{\sum_1^M \alpha^0}$)

The DFT-matrix is defined as

$$\underline{\mathbf{F}}_4 = \begin{bmatrix} 1 & 1 & 1 & 1 \\ 1 & \alpha^3 & \alpha^6 & \alpha^9 \\ 1 & \alpha^6 & 1 & \alpha^6 \\ 1 & \alpha^9 & \alpha^6 & \alpha^3 \end{bmatrix} \leftrightarrow \mathbf{F}_4 = \begin{bmatrix} 1 & 1 & 1 & 1 \\ 1 & -5 & -1 & 5 \\ 1 & -1 & 1 & -1 \\ 1 & 5 & -1 & -5 \end{bmatrix}.$$

As in a traditional OFDM system, due to the cyclic prefix, a transmission channel

$$H(z^{-1}) = 1 + 2z^{-1} - z^{-2} \leftrightarrow \underline{H}(z^{-1}) = 1 + \alpha z^{-1} + \alpha^6 z^{-2}$$

can be diagonalized using the GF DFT matrices yielding

$$\begin{aligned} \underline{\tilde{\mathbf{E}}} &= \underline{\mathbf{F}}_M \underline{\tilde{\mathbf{H}}} \underline{\mathbf{F}}_M^{-1} \\ &= \begin{bmatrix} \alpha^1 & & & \\ & \alpha^9 & & \\ & & \alpha^7 & \\ & & & \alpha^6 \end{bmatrix} \end{aligned} \quad \leftrightarrow \quad \begin{aligned} \tilde{\mathbf{E}} &= \left(\mathbf{F}_M \tilde{\mathbf{H}} \mathbf{F}_M^{-1}\right)_{13} \\ &= \begin{bmatrix} 2 & & & \\ & 5 & & \\ & & -2 & \\ & & & -1 \end{bmatrix} \end{aligned}$$

□

The performance of the RS-SC-CP transmission scheme will be analyzed in section IV.

III. RS-SC-CP over a non-integer channel with AWGN

If the assumption of an integer-valued channel is violated, and/or in the presence of AWGN, the situation becomes quite different. AWGN typically has a smaller energy compared to the PAM constellation. A traditional *complex field frequency domain equalizer* (FEQ) is able to reduce the noise in a particular frequency band if the corresponding one-tap equalizer coefficient is smaller than one. However, if this coefficient is larger than one, the noise is amplified, possibly causing a decision error. In the latter case, it can be better to take a decision first and perform the equalization in the GF (as in the RS-SC-CP system of the previous section). Intuitively, it is clear that the equalization can be split and an extra *complex field equalizer* $\tilde{\mathbf{W}}$ is added (see Figure 1) prior to the decision device $(\bullet)_p$. The complex field equalizer, operating in a block wise fashion on each $M \times 1$ block, can be designed based on a zero-forcing criterion, such that

$$\tilde{\mathbf{W}}\tilde{\mathbf{H}} = \tilde{\mathbf{H}}' \tag{20}$$

with $\tilde{\mathbf{H}}'$ and (consequently) $\tilde{\mathbf{W}}$ circulant matrices and such that $\tilde{\mathbf{H}}'$ is an integer matrix. The Reed-Solomon code then allows the residual ISI (in the general case where $\tilde{\mathbf{H}}' \neq \mathbf{I}$) to be canceled after decoding, by the *GF equalizer* $\underline{\tilde{\mathbf{E}}}$ now based on $\underline{\tilde{\mathbf{H}}'}$ instead of $\underline{\tilde{\mathbf{H}}}$. Note that $\tilde{\mathbf{W}}$ can be implemented in the frequency domain, just as the FEQ in a traditional OFDM scheme.

The rest of this section is devoted to the computation of the complex field equalizer $\tilde{\mathbf{W}}$, based on an MMSE criterion instead of a ZF criterion, typically leading to better solutions. According to this criterion, the following optimization problem is solved

$$\min_{\tilde{\mathbf{W}}, \tilde{\mathbf{H}}'} J = \min_{\tilde{\mathbf{W}}, \tilde{\mathbf{H}}'} \mathcal{E}\{\mathbf{e}^H \mathbf{e}\} \tag{21}$$

with $\mathcal{E}$ the expectation operator and the error

$$\mathbf{e} = \mathbf{w} - \hat{\mathbf{w}}. \tag{22}$$

The cost function is depicted in Figure 3. Here, variables $\mathbf{w}$ and $\hat{\mathbf{w}}$ are $M \times 1$ vectors corresponding to an OFDM block. This optimization problem should be solved with an integer constraint on $\tilde{\mathbf{H}}'$, and excluding the trivial solutions $\tilde{\mathbf{W}} = \tilde{\mathbf{H}}' = \mathbf{O}$. Apart from the integer constraint, this problem is a

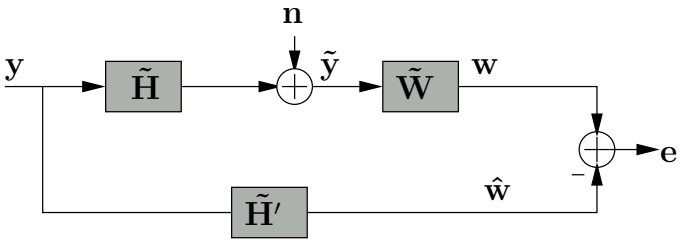

Fig. 3. Block diagram illustrating the MMSE cost function for finding $\tilde{\mathbf{W}}$.

standard linear MMSE estimation problem [11]. The noise is a zero-mean random variable, with correlation matrices

$$\mathbf{R}_{\mathbf{n}} = \mathcal{E}\{\mathbf{n}\mathbf{n}^H\} = \sigma_n^2 \mathbf{I}_M$$

It can be verified that there is no correlation inside a block of M transmitted symbols:

$$\mathbf{R}_{\mathbf{y}} = \mathcal{E}\{\mathbf{y}\mathbf{y}^H\} = \sigma_y^2 \mathbf{I}_M = \sigma_u^2 \mathbf{I}_M$$

This can be seen as follows: Each randomly chosen vector $\mathbf{u}$ of $\kappa \geq M$ symbols of a codeword of a RS code is uniformly distributed, since an equivalent (systematic) RS code can always be found that maps $\mathbf{u}$ onto the codeword [12]. In conclusion, the *different blocks* $\mathbf{y}$ are correlated (due to the RS code), but there is no correlation between the symbols inside an OFDM block.

With $\tilde{\mathbf{y}} = \tilde{\mathbf{H}}\mathbf{y} + \mathbf{n}$, the correlation matrix

$$\mathbf{R}_{\tilde{\mathbf{y}}} = \mathcal{E}\{\tilde{\mathbf{y}}\tilde{\mathbf{y}}^H\} \tag{23}$$

and the cross correlation matrix

$$\mathbf{R}_{\hat{\mathbf{w}}\tilde{\mathbf{y}}} = \mathcal{E}\{\hat{\mathbf{w}}\tilde{\mathbf{y}}^H\} \tag{24}$$

the MMSE for $\tilde{\mathbf{W}}$ assuming $\tilde{\mathbf{H}}'$ is given can be written as [11, Section 2.1]

$$\tilde{\mathbf{W}} = \mathbf{R}_{\hat{\mathbf{w}}\tilde{\mathbf{y}}}\mathbf{R}_{\tilde{\mathbf{y}}}^{-1} = \tilde{\mathbf{H}}'\mathbf{R}_{\mathbf{y}\tilde{\mathbf{y}}}\mathbf{R}_{\tilde{\mathbf{y}}}^{-1}. \tag{25}$$

With

$$\mathbf{R}_{\hat{\mathbf{w}}} = \mathcal{E}\{\hat{\mathbf{w}}\hat{\mathbf{w}}^H\} = \tilde{\mathbf{H}}'\mathbf{R}_y\tilde{\mathbf{H}}'^H, \tag{26}$$

the error covariance matrix becomes

$$\begin{aligned}
\mathbf{R}_e &= \mathcal{E}\{\mathbf{e}\mathbf{e}^H\} && (27)\\
&= \mathcal{E}\{(\mathbf{w}-\hat{\mathbf{w}})(\mathbf{w}-\hat{\mathbf{w}})^H\} && (28)\\
&= \mathcal{E}\{(\mathbf{W}\tilde{\mathbf{y}}-\hat{\mathbf{w}})(\mathbf{W}\tilde{\mathbf{y}}-\hat{\mathbf{w}})^H\} && (29)\\
&= \mathbf{R}_{\hat{\mathbf{w}}} - \mathbf{R}_{\hat{\mathbf{w}}\tilde{\mathbf{y}}}\mathbf{R}_{\tilde{\mathbf{y}}}^{-1}\mathbf{R}_{\hat{\mathbf{w}}\tilde{\mathbf{y}}}^H && (30)\\
&= \tilde{\mathbf{H}}' \underbrace{\left(\mathbf{R}_{\mathbf{y}} - \mathbf{R}_{\mathbf{y}\tilde{\mathbf{y}}}\mathbf{R}_{\tilde{\mathbf{y}}}^{-1}\mathbf{R}_{\mathbf{y}\tilde{\mathbf{y}}}^H\right)}_{\mathbf{R}_s} \tilde{\mathbf{H}}'^H && (31)
\end{aligned}$$

The matrix $\mathbf{R}_s$ is often referred to as the Schur complement of $\mathbf{R}_e$ with respect to $\mathbf{R}_{\tilde{\mathbf{y}}}$.

The MMSE in Equation 21 is the trace of the error covariance matrix [11, Section 2.1]

$$\min_{\tilde{\mathbf{H}}'} J = \min_{\tilde{\mathbf{H}}'} \mathrm{Tr}(\mathbf{R}_e), \tag{32}$$

subject to $\tilde{\mathbf{H}}' \neq \mathbf{0}$ and integer. Assuming positive definiteness of $\mathbf{R}_e$, $\mathbf{R}_s$ will be positive definite too. Consequently, the resulting optimization problem is a mixed integer quadratic programming problem. The global optimum $J_{\min}$ of this optimization problem coincides with the trivial zero solution $\tilde{\mathbf{H}}' = \mathbf{O}$, which is excluded. Since finding an efficient algorithm to solve this problem is out of the scope of this paper, we will merely use an exhaustive search.

Example 2: If $H(z^{-1}) = 2.1412 - 0.4400z^{-1} + 4.6143z^{-2}$ and $\sigma_n = 0.3742$ (SNR=20dB), the solution of the aforementioned optimization problem is

$$\tilde{\mathbf{W}} = \begin{bmatrix} 0.1486 & 0.0097 & 0.1486 & 0.0097 \\ 0.0097 & 0.1486 & 0.0097 & 0.1486 \\ 0.1486 & 0.0097 & 0.1486 & 0.0097 \\ 0.0097 & 0.1486 & 0.0097 & 0.1486 \end{bmatrix} \tag{33}$$

$$\tilde{\mathbf{H}}' = \begin{bmatrix} 1 & 0 & 1 & 0 \\ 0 & 1 & 0 & 1 \\ 1 & 0 & 1 & 0 \\ 0 & 1 & 0 & 1 \end{bmatrix} \tag{34}$$

The corresponding $J_{\min} = 0.0249$. □

IV. Simulation results

This section compares the performance of RS-SC-CP with traditional RS coded SC-CP and OFDM transmission. The latter two schemes can be explained in terms of Figure 4. In the case of an OFDM scheme, an RS code $\mathcal{R}(\nu, \kappa)$ is concatenated with a complex field OFDM modulator for which $C_m(z^{-1})$ is defined as in Equation 3 with W_M now an M-th root of unity in the complex field $\mathbb{C}$, i.e. $W_M = e^{\frac{2j\pi}{M}}$. At the receiver, only a complex field equalizer $\tilde{\mathbf{W}} = \tilde{\mathbf{E}}^{-1}\mathbf{F}_M$ is needed, with the diagonal matrix $\tilde{\mathbf{E}}$ corresponding to the frequency domain equalization (FEQ). Posterior to this equalization, decisions are taken and the resulting codeword in the GF is decoded with a Berlekamp-Massey RS decoder.

In the SC-CP case, the IDFT operation at the transmitter is shifted to the receiver such that $C_m(z^{-1}) = z^{-m}$. The complex field equalizer $\tilde{\mathbf{W}} = \tilde{\mathbf{H}}^{-1}$ is a circulant matrix, and can consequently be implemented in the frequency domain:

$$\tilde{\mathbf{W}} = \tilde{\mathbf{H}}^{-1} = \mathbf{F}_M^{-1}\tilde{\mathbf{E}}^{-1}\mathbf{F}_M. \tag{35}$$

Again, the core of the SC-CP system is surrounded with an RS code $\mathcal{R}(\nu, \kappa)$ with a Berlekamp-Massey decoder.

In Figure 5, simulation results are shown. For a word error rate of 10^{-3}, the RS-SC-CP scheme based on the RS code $\mathcal{R}(12, 8)$ (as introduced in example 1) using a 13-PAM constellation performs approximately 8dB better than a classical (complex field) OFDM scheme concatenated with the same $\mathcal{R}(12, 8)$ code. Likewise, performance results of an RS coded SC-CP system as well as an RS coded system with flat fading are shown (both using a 13-PAM constellation). The RS-SC-CP and coded OFDM/SC-CP scheme use a 3-tap Rayleigh fading channel, resulting in a 50% cyclic prefix overhead. In the next example, a more realistic case with a longer RS code and a small cyclic prefix overhead is presented. As a second remark, note that in the OFDM case, the transmitted symbols (and the AWGN) are complex valued, thereby exploiting an extra degree of freedom in favor of the OFDM case. Again, we refer to the next example where all constellations are complex valued.

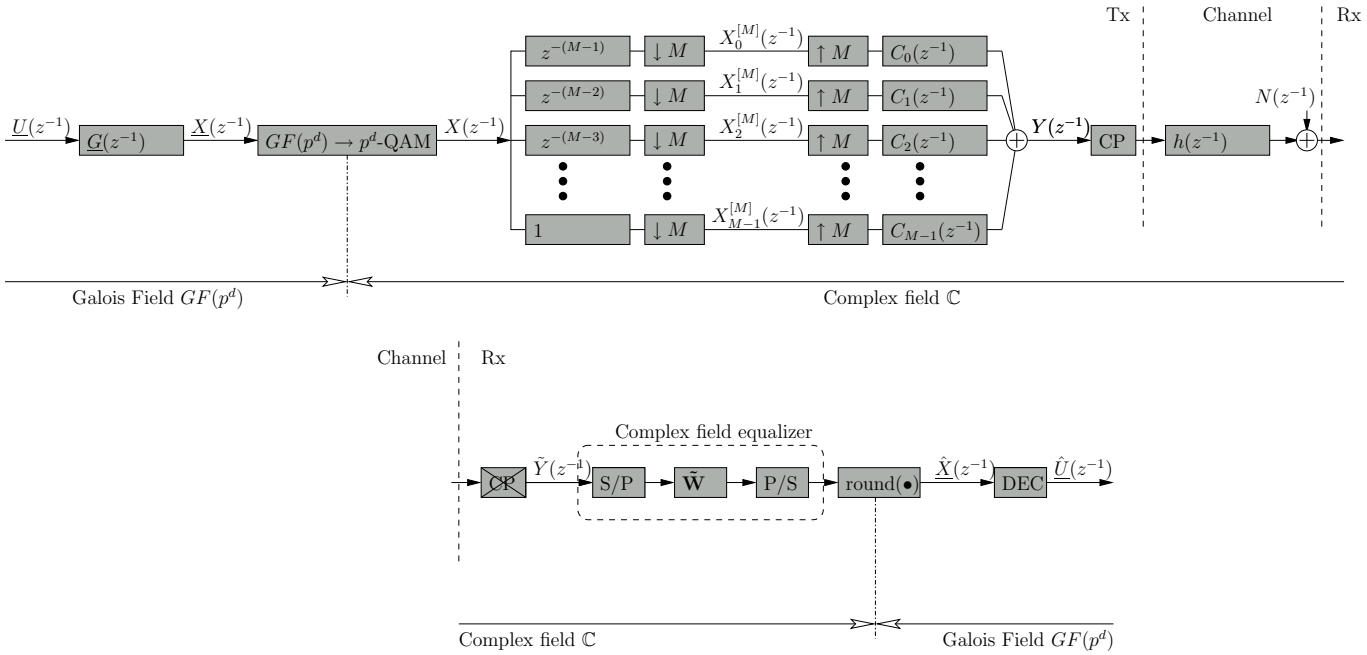

Fig. 4. Transmultiplexer structure of a baseband discrete-time model of an RS coded OFDM/SC-CP system.

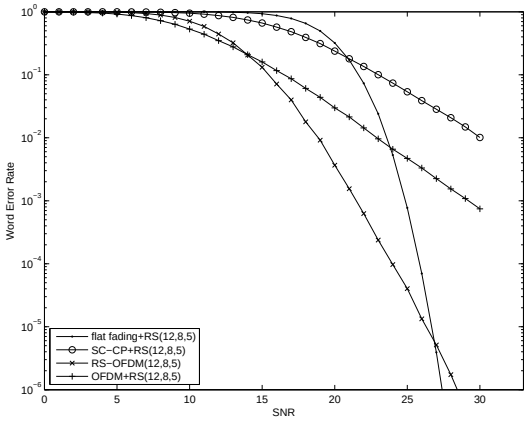

Fig. 5. Comparison of a concatenated scheme of $\mathcal{R}(12, 8)$ followed by an OFDM or SC-CP modulator and the RS-SC-CP scheme based on $\mathcal{R}(12, 8)$. The RS-SC-CP scheme has an overall Hamming distance of 6 compared to 2 for the concatenated schemes.

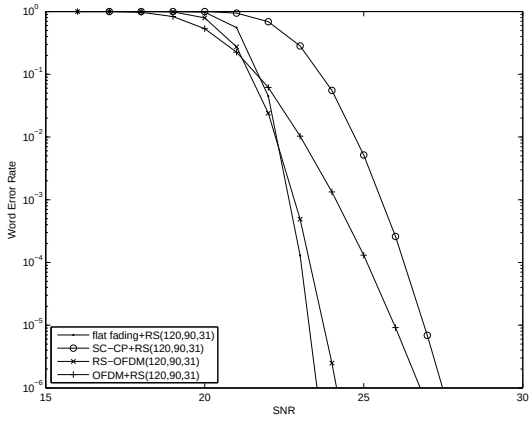

Fig. 6. Comparison of a concatenated scheme of $\mathcal{R}(120, 90)$ followed by an OFDM or SC-CP modulator and the RS-SC-CP scheme based on $\mathcal{R}(120, 90)$. The RS-SC-CP scheme has an overall Hamming distance of 6 compared to 2 for the concatenated schemes.

Simulation results using the the RS code $\mathcal{R}(120, 90)$ can be found in Figure 6. The constellation is a square 121-QAM constellation. This time, a Rayleigh fading 4-tap channel $H(z^{-1})$ is chosen. The gain of RS-SC-CP over coded OFDM amounts to approximately 2.5dB (at a word error rate of 10^{-6}) and increases with decreasing word error rate.

V. Conclusion

In this paper, the RS-SC-CP scheme is presented, in which the circulant channel matrix is diagonalized using DFT matrices in a GF rather than in the complex field. More importantly, these DFT matrices operate as the synthesis bank of a filter bank representation of an RS code. In order to be compatible with the finite field operations, the channel is first assumed to be quantized and a decision device including a modulo operation must be added at the receiver. In the case of impulse noise, this modulo operation was found not to compromise system performance [1].

For the more realistic scenario with AWGN and non-integer channel coefficients, a modified RS-SC-CP system is presented in which the equalization is split in two stages: the first stage encompasses a partial equalization in the complex field, avoiding noise amplification. This equalizer also ensures that the residual channel response has integer coefficients. It is calculated using an MMSE criterion. In the second stage, the residual ISI as well as the remaining noise is removed by the Reed-Solomon decoder followed by a GF equalizer. The performance of the RS-SC-CP system is further evaluated by simulation results showing a significant performance gain of the RS-SC-CP system compared to classical coded OFDM/SC-

CP schemes.

APPENDIX
p^2-QAM CONSTELLATIONS

In this paper, Galois fields of order p were used which are isomorphic to p-PAM constellations $-\frac{p-1}{2}..\frac{p-1}{2}$. It is well known that QAM constellations have a better performance due to an extra degree of freedom. The goal of this appendix is to find an isomorphism between Galois fields $GF(p^2)$ and QAM constellations.

QAM constellations are a subset of $\mathbb{C}$. The field of complex numbers is an extension field of the field of real numbers $\mathbb{R}$, denoted as $\mathbb{C} = \mathbb{R}^2$, where $\mathbb{R}$ is referred to as the base field. Any member of $\mathbb{C}$ can be written as a 2-tuple of elements in $\mathbb{R}$, or a polynomial with coefficients in $\mathbb{R}$:

$$[a, b] \leftrightarrow a + bx \tag{36}$$

Addition in $\mathbb{C}$ can simply be defined as addition of the polynomials. To define multiplication, an irreducible polynomial $\Pi(x) = 1 + x^2$ with coefficients in $\mathbb{R}$ is specified. Multiplication can now be defined modulo $\Pi(x)$. This leads to the following (well-known) arithmetic:

$$[a, b] \cdot [c, d] = [a \cdot c - b \cdot d, a \cdot d + b \cdot c] \tag{37}$$

$$[a, b] + [c, d] = [a + c, b + d] \tag{38}$$

Defining $j \in \mathbb{C}$ as the residue class of the element $[0, 1]$, it follows that $\Pi(j) = 0$ or $j^2 = -1$. Hence, this 'special' element $j \in \mathbb{C}$, $j \notin \mathbb{R}$ is often used in the polynomial representation leading to the notation $a+bj$ instead of $a+bx$. Note that other representations are possible, e.g. multiplication is easier defined by choosing an exponential representation $a + jb = re^{j\theta}$. These three representations are summarized in Table I.

TABLE I
THREE REPRESENTATIONS OF ELEMENTS IN $\mathbb{C}$.

2-tuple	polynomial	exponential
$[a, b]$	$a + jb$	$re^{j\theta}$

Equivalently, $GF(p)^d$ (also denoted as $GF(p^d)$) is an extension field of $GF(p)$, where $GF(p)$ is referred to as the base field. Any member of $GF(p^d)$ can be written as a d-tuple of elements in $GF(p)$, or a polynomial with coefficients in $GF(p)$. This polynomial representation is useful to define the multiplication in $GF(p^d)$. Indeed, by defining an irreducible polynomial $\Pi(x)$, the elements of $GF(p^d)$ can be described as residue classes of the polynomials with coefficients from $GF(p)$, reduced modulo $\Pi(x)$. Defining α as the residue class of the element $[0, 1, 0, ..., 0]$, it follows that $\Pi(\alpha) = 0$. If $\Pi(x)$ is also primitive, all the nonzero elements of $GF(p^d)$ form a cyclic group of order $p^d - 1$. I.e. any nonzero element can be written uniquely as a power of α. In conclusion, each element of $GF(p^d)$ can be written as a d-tuple, as a polynomial or as a power of α.

Example 3: In this example, $GF(3)$ is chosen as the base field. Addition and multiplication are therefore defined modulo 3. Choosing an (irreducible) primitive polynomial in $GF(3)$

$$\Pi(x) = x^2 + x + 2 \tag{39}$$

the field $GF(3^2)$ can be constructed as shown in Table II.

TABLE II
THREE REPRESENTATIONS OF ELEMENTS IN $GF(3^2)$ DEFINED BY $\Pi(x) = x^2 + x + 2$.

2-tuple	polynomial	exponential
$[0, 0]$	0	0
$[1, 0]$	1	1
$[0, 1]$	α	α
$[1, 2]$	$1 + 2\alpha$	α^2
$[2, 2]$	$2 + 2\alpha$	α^3
$[2, 0]$	2	α^4
$[0, 2]$	2α	α^5
$[2, 1]$	$2 + \alpha$	α^6
$[1, 1]$	$1 + \alpha$	α^7

Unfortunately, $\Pi(x) = x^2 + 1$ (used to define the multiplication in $\mathbb{C}$) is not a primitive polynomial in $GF(3^2)$ since its roots α^2 and α^6 do not generate $GF(3^2)$. Therefore, another representation of $GF(3^2)$ is needed to construct the isomorphism between $GF(3^2)$ and a 9-QAM constellation. □

In fact, $GF(p^d)$ can be viewed as a vector space of dimension d over $GF(p)$. Any set λ of linearly independent elements of $GF(p)$ can serve as a basis for $GF(p^d)$. If the field is constructed using its primitive polynomial $\Pi(x)$, the normal base $\lambda = 1, \alpha, \alpha^2, ...$ is used. However, other bases can be used. Typically, the trace operation is used to switch between bases. The trace of $\gamma \in GF(p^d)$ is defined as

$$T_d(\gamma) = \sum_{j=0}^{d-1} \gamma^{p^j} \tag{40}$$

The trace of an element γ always belongs to $GF(p)$. This is a useful property for decomposing an element γ along a specified base $\lambda_0..\lambda_{d-1}$, as we will see. First, we define the complementary basis. A basis $\beta_0..\beta_{d-1}$ is said to be complementary to $\lambda_0..\lambda_{d-1}$ if

$$T_d(\beta_i \lambda_i) = \delta_{ij} \tag{41}$$

with δ_{ij} the Kronecker delta. Each element $\gamma \in GF(p^d)$ can now be written as [12]

$$\gamma = \sum_{i=0}^{d-1} T_d(\beta_i \gamma) \lambda_i \tag{42}$$

Example 4: As an example, the trace can be used to obtain the polynomial representation of $\gamma = \alpha^5 \in GF(3^2)$ defined by $\Pi(x) = x^2 + x + 2$. First, the complementary basis β of the normal base $\lambda = \begin{bmatrix} 1 & \alpha \end{bmatrix}$ is calculated:

$$\beta = \begin{bmatrix} \alpha^5 & \alpha^6 \end{bmatrix} \tag{43}$$

Now, the traces are calculated according to 40

$$T_d(\beta_0 \gamma) = T_d(\alpha^5 \cdot \alpha^5) = \alpha^5 \cdot \alpha^5 + \alpha^{5^3} \cdot \alpha^{5^3} = 0 \tag{44}$$

$$T_d(\beta_1 \gamma) = T_d(\alpha^6 \cdot \alpha^5) = \alpha^6 \cdot \alpha^5 + \alpha^2 \cdot \alpha^{5^3} = \alpha^4 = 1 \tag{45}$$

Using Equation 42 and Table II, it is easily verified that $\alpha^5 = 0 \cdot \alpha^0 + 2 \cdot \alpha^1$. □

A special basis transformation unveils the isomorphism between the field $GF(p^2)$ and a p^2-QAM constellation:

Theorem 1: The isomorphism between the field $GF(p^2)$ and a p^2-QAM constellation is defined by the basis $\boldsymbol{\lambda} = \begin{bmatrix}1 & \alpha^n\end{bmatrix}, n = (p^2-1)/4$.

Proof: The theorem can be proved by demonstrating that $\alpha^{n^2} = -1\lambda_0 + 0\lambda_1$. Since $\alpha^{2n} \cdot \alpha^{2n} = \alpha^{p^2-1} = 1$ and $n \neq 0$, α^{2n} must be -1. Note that (p^2-1) is always a multiple of 4 since $(p^2-1) = (p-1)(p+1)$ and both factors are even (since p is prime). ■

Note that the isomorpism might not exist since the elements of the basis $\begin{bmatrix}1 & \alpha^n\end{bmatrix}$ must be linearly independent. For example, in $GF(5^2)$, $n = 6$ and $\boldsymbol{\lambda} = \begin{bmatrix}1 & \alpha^6\end{bmatrix}$. However, since $\alpha^0 + \alpha^0 = \alpha^6$, this is not a valid basis and so the isomorphism does not exist. It can be proved that the isomorphism exists if and only if $p+1$ does not divide n.

Example 5: We continue our example of $GF(3^2)$ with primitive polynomial in $GF(3)$

$$\Pi(x) = x^2 + x + 2 \tag{46}$$

Since $p + 1 = 4$ does not divide $n = 2$, the isomorphism exists. With a new basis $\boldsymbol{\lambda} = \begin{bmatrix}1 & \alpha^2\end{bmatrix}$, the field $GF(3^2)$ is shown in Table III.

TABLE III
THREE REPRESENTATIONS OF ELEMENTS IN $\mathbb{C}$.

2-tuple	polynomial	exponential
$[0,0]$	0	0
$[1,0]$	1	1
$[1,2]$	$1+2\alpha^2$	α
$[0,1]$	α^2	α^2
$[1,1]$	$1+\alpha^2$	α^3
$[2,0]$	2	α^4
$[2,1]$	$2+\alpha^2$	α^5
$[0,2]$	$2\alpha^2$	α^6
$[2,2]$	$2+2\alpha^2$	α^7

Note that $\alpha^4 = -1$. Hence, multiplication/addition of elements using the (new) polynomial representation is completely equivalent to multiplication/addition in the complex field ($\alpha^2 = j$). For example,

$$1 + 2j \cdot 2 + 2j = 1 \leftrightarrow \alpha \cdot \alpha^7 = 1 \tag{47}$$

Note that all fields of order p^d are isomorphic [12, p. 101]. We want to emphasize that the representations are different, but there is a one-to-one mapping between these representations preserving addition and multiplication. Finally, note that the elements of the base field can better be represented by $-\frac{p-1}{2}..\frac{p-1}{2}$ instead of $0..p-1$ to limit the energy of the constellation. I.e. addition and multiplication are calculated using $(\cdot)_p$ instead of modulo p.

□

REFERENCES

[1] G. Van Meerbergen, M. Moonen, and H. De Man, "Combining Reed-Solomon codes and OFDM for impulse noise mitigation: RS-OFDM," in *Proc. of the IEEE International Conference on Acoustics, Speech and Signal Processing (ICASSP), Toulouse, France*, vol. 4, May 15-19 2006, pp. 657 – 660.

[2] S. H. Han and J. H. Lee, "An overview of Peak-To-Average Power Ratio reduction techniques for multicarrier transmission," *IEEE Wireless Commun. Mag.*, vol. 12, no. 2, pp. 56–65, April 2005.

[3] K. Paterson and V. Tarokh, "On the existence and construction of good codes with Low Peak-to-Average Power ratios," *IEEE Trans. Inform. Theory*, vol. 46, no. 6, pp. 1974–1987, Sept. 2000.

[4] J. Davis and J. Jedwab, "Peak-to-mean power control in OFDM, Golay complementary sequences, and Reed-Muller codes," *IEEE Trans. Inform. Theory*, vol. 45, no. 7, pp. 2397 – 2417, Nov 1999.

[5] G. Van Meerbergen, M. Moonen, and H. De Man, "Critically subsampled filterbanks for SISO Reed-Solomon decoding," *IEEE Trans. Signal Processing*, vol. 54, no. 11, pp. 4446–4460, Nov. 2006.

[6] ——, "Filterbank Decompositions for (Non)-Systematic Reed-Solomon Codes with Applications to Soft Decoding," *IEEE Trans. Signal Processing*, vol. 55, no. 12, pp. 5681 – 5694, Dec. 2007.

[7] R. Blahut, "Transform Techniques for Error-Control Codes," *IBM J. Res. Develop.*, vol. 23, pp. 299–315, May 1979.

[8] J. L. Massey, "Shift-Register Synthesis and BCH Decoding," *IEEE Trans. Inform. Theory*, vol. 15, no. 1, pp. 122–127, Jan 1969.

[9] R. Koetter and A. Vardy, "Algebraic soft-decision decoding of Reed-Solomon codes," *IEEE Trans. Inform. Theory*, vol. 49, no. 11, pp. 2809 – 2825, Nov 2003.

[10] M. El-Khamy and R. McEliece, "Iterative algebraic soft-decision list decoding of Reed-Solomon codes," *IEEE J. Select. Areas Commun.*, vol. 24, no. 3, pp. 481 – 490, March 2006.

[11] A. H. Sayed, *Fundamentals of Adaptive Filtering*. John Wiley & Sons, NY, 2003.

[12] N. Sloane and F. MacWilliams, *The Theory of Error Correcting Codes*. North-Holland, Amsterdam, 1977.

Geert Van Meerbergen Geert Van Meerbergen received the Electrical Engineering degree and the Phd degree from the Katholieke Universiteit Leuven (KULeuven), Leuven, Belgium, in 2001 and 2006 respectively. He received the best student paper award at the 25th Symposium on Information Theory in the Benelux in 2004. His research interests are in the area of code theory and signal processing algorithms for communications.

Marc Moonen Marc Moonen received the electrical engineering degree and the PhD degree in applied sciences from Katholieke Universiteit Leuven, Leuven, Belgium, in 1986 and 1990 respectively. Since 2004 he is a Full Professor at the Electrical Engineering Department of Katholieke Universiteit Leuven, where he is currently heading a research team of 16 PhD candidates and postdocs, working in the area of signal processing for digital communications, wireless communications, DSL and audio signal processing. He received the 1994 K.U. Leuven Research Council Award, the 1997 Alcatel Bell (Belgium) Award (with Piet Vandaele), the 2004 Alcatel Bell (Belgium) Award (with Raphael Cendrillon), and was a 1997 'Laureate of the Belgium Royal Academy of Science'. He was chairman of the IEEE Benelux Signal Processing Chapter (1998-2002), and is currently a EURASIP AdCom Member (European Association for Signal, Speech and Image Processing, 2000-.). He has been a member of the editorial board of 'IEEE Transactions on Circuits and Systems II' (2002-2003). He is currently Editor-in-Chief for the 'EURASIP Journal on Applied Signal Processing' (2003-.), and a member of the editorial board of 'Integration, the VLSI Journal', 'EURASIP Journal on Wireless Communications and Networking', and 'IEEE Signal Processing Magazine'.

Hugo De Man Hugo De Man is professor in Electrical Engineering at the Katholieke Universiteit Leuven (KULeuven), Belgium, since 1976. He was visiting associate professor at U.C. Berkeley in 1975, teaching semiconductor physics and VLSI design. His early research was devoted to the development of mixedsignal, switched capacitor and DSP simulation tools as well as new topologies for high speed CMOS circuits which lead to the invention of NORA CMOS. In 1984, he was one of the co-founders of IMEC (Interuniversity Micro-Electronics Center), which, today, is the largest independent semiconductor research institute in Europe with over 1100 employees. From 1984-1995, he was Vice-President of IMEC, responsible for research in design technology for DSP and telecom applications. In 1995, he became a senior research fellow of IMEC, working on strategies for education and research on design of future post-PC systems. His research at IMEC has lead to many novel tools and methods in the area of high level synthesis, hardware-software co-design and C++ based design. Many of these tools are now commercialized by spin-off companies like Coware, Adelante Technologies and Target Compilers. His work and teaching also resulted in a cluster of DSP oriented companies in Leuven, now known as DSP valley, where more than 1500 DSP engineers work on design tools and on telecom, networking and multimedia integrated system products. In 1999, he received the Technical Achievement Award of the IEEE Signal Processing Society, the Phil Kaufman Award of the EDA Consortium, and the Golden Jubilee Medal of the IEEE Circuits and Systems Society. Hugo De Man is an IEEE Fellow and a member of the Royal Academy of Sciences in Belgium.